

Adenovirus E1B 55-kilodalton protein targets SMARCAL1 for degradation during infection and modulates cellular DNA replication

Nazeer, Reshma; Qashqari, Fadi; Albalawi, Abeer; Piberger, Ann Liza; Tilotta, Maria; Read, Martin; Hu, Siyuan; Davis, Simon; McCabe, Christopher; Petermann, Eva; Turnell, Andrew

DOI:

[10.1128/JVI.00402-19](https://doi.org/10.1128/JVI.00402-19)

License:

None: All rights reserved

Document Version

Peer reviewed version

Citation for published version (Harvard):

Nazeer, R, Qashqari, F, Albalawi, A, Piberger, AL, Tilotta, M, Read, M, Hu, S, Davis, S, McCabe, C, Petermann, E & Turnell, A 2019, 'Adenovirus E1B 55-kilodalton protein targets SMARCAL1 for degradation during infection and modulates cellular DNA replication', *Journal of virology*, vol. 93, no. 13, e00402-19.
<https://doi.org/10.1128/JVI.00402-19>

[Link to publication on Research at Birmingham portal](#)

Publisher Rights Statement:

Checked for eligibility: 09/05/2019

This document is the Author Accepted Manuscript version of a published work which appears in its final form in *Journal of virology*, copyright © 2019 American Society for Microbiology. The final Version of Record can be found at: <https://doi.org/10.1128/JVI.00402-19>

General rights

Unless a licence is specified above, all rights (including copyright and moral rights) in this document are retained by the authors and/or the copyright holders. The express permission of the copyright holder must be obtained for any use of this material other than for purposes permitted by law.

- Users may freely distribute the URL that is used to identify this publication.
- Users may download and/or print one copy of the publication from the University of Birmingham research portal for the purpose of private study or non-commercial research.
- User may use extracts from the document in line with the concept of 'fair dealing' under the Copyright, Designs and Patents Act 1988 (?)
- Users may not further distribute the material nor use it for the purposes of commercial gain.

Where a licence is displayed above, please note the terms and conditions of the licence govern your use of this document.

When citing, please reference the published version.

Take down policy

While the University of Birmingham exercises care and attention in making items available there are rare occasions when an item has been uploaded in error or has been deemed to be commercially or otherwise sensitive.

If you believe that this is the case for this document, please contact UBIRA@lists.bham.ac.uk providing details and we will remove access to the work immediately and investigate.

Adenovirus E1B-55K targets SMARCAL1 for degradation during
infection and modulates cellular DNA replication

Reshma Nazeer¹, Fadi S. I. Qashqari¹, Abeer S. Albalawi¹, Ann Liza Piberger¹,
Maria Teresa Tilotta¹, Martin L. Read², Siyuan Hu^{1,3}, Simon Davis^{1,4},
Christopher J. McCabe², Eva Petermann¹ and Andrew S. Turnell^{1*}

¹Institute of Cancer & Genomic Sciences

²Institute of Metabolism & Systems Research

College of Medical and Dental Sciences

The University of Birmingham

United Kingdom

B15 2TT

³University of Glasgow Centre for Virus Research

Glasgow

United Kingdom

G61 1QH

⁴Target Discovery Institute

Nuffield Department of Medicine

University of Oxford

United Kingdom

OX3 7FZ

* Author for correspondence: Andrew S Turnell

Telephone: +44-121-414-9164

e-mail: A.S.Turnell@bham.ac.uk

Running title: Adenovirus and ATR signalling pathways

Abstract: 182 words

Main text: 5966 words

38 **Abstract**

39 Here we show that the cellular DNA replication protein and ATR substrate, SMARCAL1, is
40 recruited to viral replication centres early during adenovirus infection and is then targeted in
41 an E1B-55K/E4orf6 and Cullin Ring Ligase-dependent manner for proteasomal degradation.
42 In this regard we have determined that SMARCAL1 is phosphorylated at S123, S129 and
43 S173 early during infection, in an ATR- and CDK- dependent manner, and that
44 pharmacological inhibition of ATR and CDK activities attenuates SMARCAL1 degradation.
45 SMARCAL1 recruitment to viral replication centres was shown to be largely dependent upon
46 SMARCAL1 association with the RPA complex, whilst Ad-induced SMARCAL1
47 phosphorylation also contributed towards SMARCAL1 recruitment to viral replication
48 centres, albeit to a limited extent. SMARCAL1 was found associated with E1B-55K in
49 adenovirus E1-transformed cells. Consistent with its ability to target SMARCAL1 we
50 determined that E1B-55K modulates cellular DNA replication. As such, E1B-55K expression
51 initially enhances cellular DNA replication fork-speed but ultimately leads to increased
52 replication fork stalling and the attenuation of cellular DNA replication. We propose
53 therefore, that adenovirus targets SMARCAL1 for degradation during infection to inhibit
54 cellular DNA replication and promote viral replication.

55

56

57

58

59

60 **Importance**

61 Viruses have evolved to inhibit cellular DNA damage response pathways that possess anti-
62 viral activities and utilize DNA damage response pathways that possess pro-viral activities.
63 Adenovirus has evolved, primarily, to inhibit DNA damage response pathways by engaging
64 with the ubiquitin-proteasome system and promoting the degradation of key cellular proteins.
65 Adenovirus regulates, differentially, ATR DNA damage response signalling pathways during
66 infection. The cellular, adenovirus E1B-55K binding protein, E1B-AP5, participates in ATR
67 signalling pathways activated during infection, whilst adenovirus 12 E4orf6 negates Chk1
68 activation by promoting the proteasome-dependent degradation of ATR activator, TOPBP1.
69 The studies detailed herein indicate that adenovirus utilises ATR kinase and CDKs during
70 infection to promote the degradation of SMARCAL1 to attenuate normal cellular DNA
71 replication. These studies further our understanding of the relationship between adenovirus
72 and DNA damage and cell cycle signalling pathways during infection and establish new roles
73 for E1B-55K in the modulation of cellular DNA replication.

74

75

76

77

78

79

80

81 Introduction

82 Cellular DNA damage response (DDR) signalling pathways coordinated by the
83 phosphoinositide 3-kinase (PI3K)-like kinase proteins Ataxia Telangiectasia Mutated (ATM),
84 ATM-Rad3-related gene (ATR) and DNA-dependent protein kinase (DNA-PK) are often
85 targeted by viruses during infection in order to facilitate viral replication (1, 2). As such,
86 viruses often exploit the ubiquitin-proteasome system to inhibit DDR pathway components
87 that possess anti-viral activities, and utilize DDR pathway components that possess pro-viral
88 activities (1, 3). In this regard adenovirus (Ad) types from all groups have evolved, almost
89 exclusively, to inhibit DDR pathways during infection. Early work determined that Ad5 E1B-
90 55K and E4orf6 assemble an Ad ubiquitin (Ub) ligase complex consisting of Cullin Ring
91 Ligase 5 (CRL5), Elongin B, Elongin C and Rbx1 that was capable of promoting the specific
92 degradation of the tumour suppressor gene product, p53 during infection (4, 5). In this regard
93 BC box motifs within E4orf6 served to recruit CRL5 through association with Elongins B
94 and C, whereas E1B-55K served to recruit p53 to the Ad Ub ligase through interaction with
95 E4orf6 (6). Later studies indicated that group A viruses, such as Ad12, utilized CRL2 to
96 promote the degradation of p53 during infection (7, 8).

97 The Ad Ub ligase was subsequently shown to inhibit the ATM-coordinated response to viral
98 infection by promoting the degradation of MRE11 and BLM to ensure that viral genome
99 processing, resection, recombination and concatenation are all negated (9, 10). Adenovirus
100 was also shown to inhibit non-homologous end-joining pathways coordinated by DNA-PK by
101 targeting DNA ligase IV for Ad Ub ligase-mediated degradation that also served to prevent
102 viral genome concatenation (11). The Ad Ub ligase has also been shown to promote the
103 degradation of cellular proteins not involved in DDR signalling but do, nevertheless, possess
104 anti-viral activities. As such cellular proteins involved in cell signalling, cell adhesion and

105 cell-contacts such as integrin $\alpha 3$, ALCAM, EPHA2 and PTPRF are all targeted for
106 degradation during infection (12, 13). E1B-55K can also, in isolation, promote the
107 proteasomal-mediated degradation of Daxx, a component of PML nuclear bodies and
108 transcriptional regulator that has antiviral activities (14), whilst Ad E4orf3 which possesses
109 inherent SUMO ligase activity can target cellular proteins such as TIF1 γ and TFII-I for
110 SUMO-targeted ubiquitin ligase (STUbL) -mediated degradation during infection (15-17).

111 The ATR kinase serves specifically to regulate pathways that control DNA replication in
112 response to replication stress (18). ATR is an essential gene; hypomorphic mutations cause
113 Seckel syndrome that is a pleiotropic disease characterized primarily by growth retardation
114 and microcephaly (18). ATR signalling pathways are targeted, specifically, during Ad
115 infection. It has long been known that the single-stranded (ss)DNA-binding protein complex,
116 RPA, which participates in ATR signalling pathways through its association with ssDNA
117 during cellular DNA replication and following resection at double-stranded (ds)DNA breaks
118 (DSBs), is recruited to viral replication centres (VRCs) during Ad infection and presumably
119 associates with viral ssDNA replication intermediates during genome replication (19, 20). As
120 such RPA has often served as a surrogate marker for VRCs. More recently, a number of ATR
121 signalling components required for ATR activation such as, ATR-interacting protein
122 (ATRIP), and components of the RAD9-HUS1-RAD1 (9-1-1) clamp complex and Rad17,
123 have all been shown to be recruited to VRCs following both Ad5 and Ad12 infection (19,
124 20). It has also been suggested that Ad5, but not Ad12, inhibits the ATR-dependent activation
125 of Chk1 by promoting the E4orf3-dependent immobilisation of the MRE11-RAD50-NBS1
126 complex in nuclear tracks, whilst Ad12 E4orf6 alone associates with CRL2-Rbx1 to promote
127 the degradation of the ATR activator, TOPBP1, and ensures that Chk1 is not activated during
128 Ad12 infection (7, 20). It has been determined that the ATR pathway is differentially
129 regulated during Ad infection. ATR kinase has been shown to be activated during both Ad5

130 and Ad12 infection and that the cellular Ad E1B-55K associated protein, E1B-AP5
131 (hnRNPUL1), is required for ATR activation in these circumstances (20). Indeed, E1B-AP5
132 was shown to be required for the ATR-dependent phosphorylation of RPA32 during infection
133 and also contributed towards the Ad-induced phosphorylation of Smc1 and H2AX. It is not
134 however, apparent why ATR kinase activity is not fully inactivated during Ad infection, and
135 suggests that the virus might promote the selective ATR-dependent phosphorylation of
136 specific substrates during infection to inhibit cellular replication and facilitate viral
137 replication (20).

138 SMARCAL1 (SWI/SNF-related matrix-associated actin-dependent regulator of chromatin
139 subfamily A-like protein 1) is a DNA-dependent ATPase and ATP-dependent annealing
140 helicase that has the capacity to interact with both dsDNA and ssDNA through DNA-
141 binding-domains (DBDs) within its primary structure and its interaction with the RPA
142 complex, respectively (21-25). Bi-allelic inactivation of SMARCAL1 causes Schimke
143 immuno-osseous dysplasia (SIOD) which is characterized by renal failure, immune
144 deficiencies, bone growth retardation, and predisposition to different types of cancer (26).
145 SMARCAL1 has the capacity to remodel replication forks and serves to prevent replication
146 fork collapse and promote replication restart (21-25). As such SMARCAL1 is recruited to
147 stalled forks through its interaction with RPA to promote fork regression and the restoration
148 of fork structure. SMARCAL1 function is regulated by the ATR kinase; in response to
149 replication stress ATR phosphorylates SMARCAL1 on S652 and limits its fork regression
150 and fork processing activities (27). Indeed, when ATR is inhibited pharmacologically such
151 that SMARCAL1 activity is not tightly regulated, uncoordinated SMARCAL1 activity
152 promotes fork collapse (28). SMARCAL1 also participates directly in response to different
153 types of DNA damage and is recruited in an RPA-dependent manner to DSBs that have been

154 processed to generate ssDNA, and serves to both stabilize replication forks, and restore fork
155 integrity (21-25).

156 As our understanding of the relationship between ATR signalling pathways and adenovirus is
157 incomplete this study sought to further our knowledge in this area. As such we determined
158 that the ATR substrate, SMARCAL1 is phosphorylated in ATR and CDK-dependent manner
159 and then targeted for degradation during adenovirus infection to presumably to disable its
160 cellular activities during infection. Consistent with this notion, E1B-55K, which associates
161 specifically with SMARCAL1, was shown to dysregulate cellular DNA replication fork
162 speed and promote replication fork stalling. We propose therefore that adenovirus inhibits
163 SMARCAL1 activity to effectively inactivate cellular DNA replication during infection.

164

165 **Materials and Methods**

166 **Cells.** A549 human lung carcinoma cells, TERT-immortalized RPE-1 (retinal pigment
167 epithelial) cells, FlpIn T-REX U2OS cells and GP2-293 cells were grown in HEPES-
168 modified Dulbecco's modified Eagle's medium (DMEM; Sigma-Aldrich) supplemented with
169 8% (v/v) foetal calf serum (FCS; Sigma-Aldrich) and 2 mM L-glutamine (Sigma-Aldrich).
170 Ad5 and Ad12 E1B-55K FlpIn T-Rex U2OS cells were maintained in HEPES-modified
171 DMEM media in the presence of 200µg/ml Hygromycin (Life Technologies), whilst clonal
172 RPE-1 cells that express wild-type (*wt*) GFP-SMARCAL1 or GFP-SMARCAL1 mutants
173 were also maintained in HEPES-modified DMEM media in the presence of 500µg/ml G418
174 (Gibco). All cells were maintained at 37 °C in a humidified 5% CO₂ atmosphere (Nuaire
175 Autoflow).

176 **Viruses.** *wt* Ad5 and *wt* Ad12 Huie viruses were from the ATCC. Ad5 *dl1520*, Ad5 *pm4150*,
177 Ad5 *pm4154* Ad5 *pm4155* and Ad12 *dl620* viruses have all been described previously (15).
178 Ad5 and Ad12 viruses were propagated on permissive human embryonic kidney (HEK) 293
179 cells and human embryonic retinoblastoma (HER) 3 cells, respectively, and titres determined
180 by plaque assay on HER911, and HER3 cells, respectively. Viruses were diluted in DMEM
181 without FCS and cells were typically infected at a multiplicity of infection (MOI) of 10.
182 Infected cells were incubated at 37 °C with agitation every 10 minutes. After 2 hours
183 infection, virus-containing medium was removed and replaced with fresh culture medium
184 supplemented with 8% (v/v) FCS.

185 **Plasmids.** *wt* SMARCAL1 and Δ N-SMARCAL1 (lacking the N-terminal RPA-interaction
186 domain; Δ RPA) constructs cloned into the retroviral vector pLEGFP-C1 (Clontech) were
187 provided by Dr David Cortez. pLEGFP-C1 S123A, S129A and S173A SMARCAL1
188 phospho-mutants were generated using the QuikChange II XL site-directed mutagenesis kit
189 (Agilent) and validated by Sanger sequencing. Using *wt* Ad5 E1B-55K and Ad12 E1B-55K
190 cDNA templates both Ad5 and Ad12 E1B-55K were amplified by PCR, digested with
191 BamHI and XhoI, and sub-cloned into the pcDNA5/FRT/TO plasmid for the generation of
192 TET-inducible cell lines. Ad5 E1B-55K was amplified using the primers: Ad5 E1B55K
193 BamHI Forward: AGGTTGGATCCATGGAGCGAAGAAACCCATCTGAG and Ad5
194 E1B55K XhoI Reverse: AGGTTCTCGAGTCAATCTGTATCTTCATCGCTAGA. Ad12
195 E1B-55K was amplified using the primers: Ad12 E1B55K BamHI Forward:
196 TTGCAGGATCCATGGAGCGAGAAATCCACCTGAG and Ad12 E1B55K XhoI
197 Reverse: TTGCACTCGAGTCAGTTGTCGTCTTCATCACTTGA. Clones were validated
198 by Sanger sequencing using the primers pcDNA5 Forward:
199 CGCAAATGGGCGGTAGGCGTG; pcDNA5 Reverse: TAGAAGGCACAGTCGAGG;
200 Ad5 E1B-55K seq1: GGCTACAGAGGAGGCTAGGAATCTA; Ad5 E1B-55K seq2:

201 CCTGGCCAATACCAACCTTATCCT; Ad5 E1B-55K seq3:
202 TGCTGACCTGCTCGGACGGCAACT; Ad12 E1B-55K seq1:
203 AACTGTATATTGGCAGGAGTTGCAG; Ad12 E1B-55K seq2:
204 AATACCTGTCTTGTCTTGCATGGT; Ad12 E1B-55K seq3:
205 ATAACATGTTTATGCGCTGTACCAT.

206 **Generation of clonal cell lines.** FlpIn T-REX U2OS cells were grown to 90% confluence
207 prior to transfection. The Ad5 E1B-55K and Ad12 E1B-55K pcDNA5/FRT/TO plasmids
208 were mixed with the recombination plasmid, pOG44, in a 1:9 ratio in Opti-MEM (Life
209 Technologies), and transfected according to the manufacturer's instructions into FlpIn T-
210 REX U2OS cells with the use of Lipofectamine 2000 (Life Technologies). Cells were then
211 incubated in a CO₂-humidified incubator at 37°C for 6 hours. Following transfection cells
212 were incubated in fresh HEPES-modified DMEM supplemented with 8% (v/v) FCS and
213 2mM glutamine. 24 h post-transfection cells from one plate were passaged onto four plates,
214 and 48h post-transfection incubated with growth medium containing 200µg/ml Hygromycin
215 (Life Technologies) for clonal selection. Cells were then fed every three days; individual
216 colonies were ultimately selected, expanded and assessed for Ad E1B-55K expression
217 following incubation with 0.1µg/ml doxycycline for 24h. To generate GFP-SMARCAL1 cell-
218 lines, pLEGFP-C1 SMARCAL1 constructs were transfected in a 1:1 ratio with the pVSV
219 envelope plasmid in the retrovirus packaging cell line, GP2-293 cells (Clontech) using
220 Lipofectamine 2000. 72 h post-transfection, the virus-containing supernatants were collected
221 and filtered through a 0.45 µM filter (Sartorius). Retroviral transduction of RPE-1 cells, at
222 20% density, was then performed. 72 h post-transduction clonal cells were selected using
223 G418 (500 µg/ml). Individual colonies were ultimately expanded and assessed for GFP-
224 SMARCAL1 expression.

225 **Antibodies and inhibitors.** The anti-Ad5 E1B-55K monoclonal antibody (mAb), 2A6, anti-
226 Ad12 E1B-55K mAb, XPH9 and the anti-p53 mAb, DO-1 were all obtained as supernatant
227 fluid from cultures of the appropriate hybridoma cell lines. The anti-SMARCAL1 (A-2) mAb
228 was from Santa Cruz (sc-376377). Horseradish peroxidase (HRP)-conjugated secondary anti-
229 mouse and anti-rabbit antibodies used for Western blotting were from Agilent. Secondary
230 anti-mouse and anti-rabbit Alexa 488/594 antibodies used for immunofluorescence were from
231 Thermo Fisher. The ATR inhibitor, AZD6738, and the CRL inhibitor, MLN4924, were
232 purchased from Cayman chemicals, whilst the CDK inhibitor, RO-3306 was purchased from
233 Merck Millipore.

234 **Immunoprecipitation.** Cells were harvested by washing twice in ice-cold phosphate-
235 buffered saline and solubilized in immunoprecipitation (IP) buffer containing 20 mM Tris-
236 HCl (pH 8.0), 150 mM NaCl, 1 mM ethylenediaminetetraacetic acid (EDTA), 1% (v/v)
237 Nonidet P-40, 25 mM NaF and 25 mM β -glycerophosphate. Cell lysates were then
238 homogenized twice with 10 strokes while being kept on ice and centrifuged at 40000 rpm for
239 30 minutes at 4 °C. Immunoprecipitating antibodies were added to clarified supernatants at 4
240 °C overnight with rotation. After this time Protein G-Sepharose beads (Sigma-Aldrich) were
241 added to all samples to capture and isolate immune complexes for 2 hours at 4 °C with
242 rotation. The beads were then washed five times by centrifugation at 3000 rpm in ice-cold IP
243 buffer, eluted in 30 μ l of SDS-containing sample buffer and ran on SDS-PAGE gels for
244 Western blotting.

245 **SDS-PAGE and Western blot analysis.** Whole-cell protein lysates were prepared in 9M
246 urea, 150 mM β -mercaptoethanol, 50 mM Tris-HCl (pH 7.4). Lysates were clarified by
247 sonication and centrifugation, and protein concentrations determined by Bradford assay (Bio-
248 Rad). Proteins were separated by SDS-PAGE in the presence of 100 mM Tris, 100 mM

249 Bicine and 0.1% (w/v) SDS. Following SDS-PAGE, proteins were electrophoretically
250 transferred onto nitrocellulose membranes (PALL) in transfer buffer (50 mM Tris, 190 mM
251 glycine, 20% (v/v) methanol). Membranes were then blocked in 5% (w/v) dried milk powder
252 in TBST (Tris-buffered saline containing 0.1% (v/v) Tween-80) for 1 h at room temperature
253 with agitation. Membranes were incubated overnight with antibodies at the appropriate
254 dilution in TBST containing 5% (v/v) milk at 4 °C with agitation. The following day,
255 membranes were washed four times in TBST and incubated with the appropriate HRP-
256 conjugated secondary antibody made up in TBST containing 5% (v/v) milk at room
257 temperature for 2 hours with agitation. Finally, membranes were washed four times in TBST
258 and antigens were detected using enhanced chemiluminescence (ECL) reagents (Millipore)
259 and autoradiography film (SLS).

260 **Microscopy.** GFP-SMARCAL1 cells were visualised using an EVOS Fluorescent digital
261 inverted microscope. Cells for confocal microscopy were seeded on glass 12-well multi-spot
262 microscope slides (Hendley-Essex). Following mock or Ad infection slides were fixed in 4%
263 (w/v) paraformaldehyde in PBS then permeabilized in ice-cold acetone. Slides were then air-
264 dried, and blocked in HINGS buffer (20% (v/v) Heat-Inactivated Normal Goat Serum, 0.2%
265 (w/v) BSA in PBS), prior to incubation with the appropriate primary, and Alexa Fluor®
266 secondary antibodies (Life Technologies) in HINGS buffer. Slides were then mounted in
267 Vectashield (Vector Laboratories) containing 4',6-diamidino-2-phenylindole (DAPI) and
268 visualized using an LSM 510 META confocal laser scanning microscope (Carl Zeiss).

269 **Mass Spectrometry.** Anti-SMARCAL1 immunoprecipitates were isolated on Protein G
270 Sepharose beads and separated upon pre-cast Novex NuPage™ 4-12% Bis-Tris Gels (Life
271 Technologies). Protein bands were stained with colloidal Coomassie Brilliant Blue (Fisher).
272 After washing gels in distilled water protein bands were excised and washed twice, by

273 agitation, with a solution containing 50 mM ammonium bicarbonate and 50% (v/v)
274 acetonitrile for 45 min at 37°C. The excised proteins were then reduced by incubation for 1 h
275 at 56°C in a solution containing 50 mM dithiothreitol and 50 mM ammonium bicarbonate in
276 10% (v/v) acetonitrile. Proteins were then incubated in an alkylating solution (200 mM
277 iodoacetamide, 50 mM ammonium bicarbonate, and 10% (v/v) acetonitrile) for 30 min at
278 room temperature in the dark. The protein bands were then washed three times for 15 min
279 each at room temperature in 10% (v/v) acetonitrile /40 mM ammonium bicarbonate on a
280 shaker, and then dried in a DNA–mini-vacuum centrifuge for 3-4 h. The dried samples were
281 then resuspended and digested by rehydration in sequence-grade modified trypsin (Promega).
282 An equal volume of 10% (v/v) acetonitrile/40mM ammonium bicarbonate was then added to
283 the protein bands and left to incubate with agitation overnight at 37°C. The resultant peptides
284 were then analyzed using a Q Exactive™ HF Hybrid Quadrupole-Orbitrap™ Mass
285 Spectrometer (ThermoFisher Scientific).

286 **DNA fibre analysis.** Cells were labelled with 25 µM CldU (Sigma-Aldrich) and 250 µM IdU
287 (Sigma-Aldrich) for 20 min each and DNA fibre spreads prepared in 200 mM Tris-HCl pH
288 7.4, 50 mM EDTA, 0.5% (w/v) SDS and fixed with a 3:1 mixture of methanol/acetic acid.
289 DNA fibre spreads were then denatured with 2.5 M HCl for 80 mins then incubated with
290 blocking buffer (PBS + 1% (w/v) BSA + 0.1% (v/v) Tween20) for 1 h prior to incubation
291 with rat anti-BrdU (BU1/75, Abcam ab6326, 1:250) and mouse anti-BrdU (B44, Becton
292 Dickinson 347580, 1:500) in blocking buffer for 1 h. Fibres were then fixed with 4% (w/v)
293 paraformaldehyde and incubated further with anti-rat AlexaFluor 555 and anti-mouse
294 AlexaFluor 488 for 1.5 h prior to mounting and analysis on a Nikon E600 microscope with a
295 Nikon Plan Apo 60x (1.3 NA) oil lens, a Hamamatsu digital camera (C4742-95) and the
296 Volocity acquisition software (Perkin Elmer). Images were analyzed using ImageJ.

297

298 **Results**299 **SMARCAL1 localizes to Ad replication centres during the early stages of infection.** As

300 we and others have shown that the RPA complex and other components of ATR signalling

301 pathways are recruited to VRCs during infection we decided initially to determine whether

302 SMARCAL1, a known ATR substrate and RPA-binding protein, was also recruited to VRCs

303 following infection of human A549 cells with either *wt* Ad5 or *wt* Ad12. Confocal

304 microscopy revealed that like RPA complex component, RPA2, SMARCAL1 was distributed

305 predominantly, throughout the nucleus in mock-infected, interphase A549 cells, although

306 there did also appear to be a proportion of cytoplasmic SMARCAL1 (panels i-iii, Figure 1).

307 Following infection with either *wt* Ad5, or *wt* Ad12, and consistent with previous studies

308 RPA2 re-localized to VRCs (panels iv-vi, Ad5; panels vii-ix, Ad12; Figure 1). Importantly,

309 SMARCAL1 was also recruited to VRCs, and co-localized with RPA2, following either *wt*310 Ad5, or *wt* Ad12 infection (panels iv-vi, Ad5; panels vii-ix, Ad12; Figure 1). Interestingly,

311 the levels of SMARCAL1 in the Ad12-infected cells appeared to be reduced relative to

312 mock-infected cells (cf panel ii (mock) with panel viii (Ad12), Figure 1). Taken together

313 these data indicate that SMARCAL1 is recruited to VRCs during Ad infection.

314 **SMARCAL1 protein levels are reduced following Ad5 and Ad12 infection.** Given that the

315 immunofluorescence studies suggested that SMARCAL1 levels were reduced following

316 Ad12 infection (Figure 1) we next sought to determine whether absolute SMARCAL1 protein

317 levels are affected by viral infection. To do this we infected A549 cells with either *wt* Ad5 or318 *wt* Ad12 and analysed SMARCAL1 protein levels at various stages post-infection. Western

319 Blot (WB) analyses revealed that akin to p53, SMARCAL1 protein levels were reduced

320 substantially following *wt* Ad5 infection (Figure 2A). WB analyses revealed that

321 SMARCAL1 protein levels were similarly reduced following *wt* Ad12 infection (Figure 2B).
322 Interestingly, WB analyses revealed that SMARCAL1 appeared to undergo post-translational
323 modification at early time-points post-infection, as judged by an apparent increase in its
324 molecular weight, following infection with either *wt* Ad5 or *wt* Ad12 (Figures 2A and 2B).
325 These data suggest that SMARCAL1 is targeted for degradation during Ad infection.

326 **SMARCAL1 is degraded during Ad infection in an E1B-55K/E4orf6- and CRL-**
327 **dependent manner.** As E1B-55K/E4orf6 complexes and, E1B-55K, E4orf3 and E4orf6
328 alone have all been implicated in the targeting of cellular proteins for degradation, we next
329 investigated which early region viral proteins were required to induce SMARCAL1
330 degradation during infection. To do this we infected A549 cells with *wt* Ad5, the E1B-55K
331 deletion mutant, Ad5 *dl*1520, the E4orf3 deletion mutant, *pm*4150 and the Ad5 E4orf6
332 deletion mutant, *pm*4154 and then analysed SMARCAL1 protein levels at 24h and 48h post-
333 infection (Figure 3A). In line with previous studies WB analyses revealed that p53
334 degradation was dependent on the expression of both E1B-55K and E4orf6 (Figure 3A).
335 Consistent with the notion that the Ad Ub ligase was also required to promote the degradation
336 of SMARCAL1 during infection WB analyses also revealed that SMARCAL1 degradation
337 was dependent upon the expression of both E1B-55K and E4orf6 (Figure 3A). Consistent
338 with a role for E1B-55K in the degradation of SMARCAL1 in Ad12-infected cells, the Ad12
339 E1B-55K deletion mutant, Ad12 *dl*620 was not as efficient as *wt* Ad12 in promoting the
340 degradation of SMARCAL1 (Figure 3B).

341 To investigate the role for cellular CRLs in the E1B-55K/E4orf6-dependent degradation of
342 SMARCAL1 we utilised the NEDD8-activating enzyme (NAE) inhibitor, MLN4924, which
343 inhibits Cullin neddylation and activation (29). As MLN4924 has been shown to be effective
344 in the low to high nM range, and moreover, has been shown to activate p53 at high nM

345 concentrations (29, 30), we used two different doses to assess its efficacy as a CRL inhibitor
346 during Ad infection. We therefore infected A549 cells with *wt* Ad5 or *wt* Ad12, then
347 subsequently incubated infected cells in the absence, or presence, of MLN4924 and analysed
348 SMARCAL1 protein levels at 24h and 48h post-infection (Figure 3C and 3D). WB analyses
349 revealed that 500nM MLN4924 reduced markedly the ability of *wt* Ad5 and *wt* Ad12 to
350 promote SMARCAL1 degradation (cf lanes 3 and 4 with lanes 11 and 12, Figures 3C and
351 3D). As noted in other studies MLN4924 treatment, in the absence of infection promoted p53
352 stabilisation, and consistent with other reports limited p53 degradation following Ad infection
353 (30; cf lanes 1 and 2 with lanes 5 and 6 and 9 and 10, Figures 3C and 3D). Pertinently
354 however, MLN4924 treatment did not affect the levels of SMARCAL1 in mock-infected
355 cells (cf lanes 1 and 2 with lanes 5 and 6 and 9 and 10, Figures 3C and 3D). Taken together
356 these data suggest that E1B-55K/E4orf6 recruit cellular CRLs to promote the degradation of
357 SMARCAL1 during Ad infection.

358 **SMARCAL1 is phosphorylated in the early stages of Ad5 and Ad12 infection.** As ATR
359 kinase is known to be activated following Ad infection and SMARCAL1 migration on SDS-
360 PAGE was retarded following infection we next investigated whether SMARCAL1 was
361 phosphorylated in response to Ad infection. To do this we first infected A549 cells with
362 either *wt* Ad5 or *wt* Ad12 then immunoprecipitated SMARCAL1 from mock-infected or Ad-
363 infected cells with an anti-SMARCAL1 antibody. Immunoprecipitates were then either left
364 untreated or treated with λ -phosphatase prior to investigating the migratory properties of
365 SMARCAL1 on SDS-PAGE. Consistent with the notion that SMARCAL1 is phosphorylated
366 following Ad infection, WB analyses revealed that when anti-SMARCAL1
367 immunoprecipitates from Ad-infected cells were treated with λ -phosphatase the migration of
368 SMARCAL1 was increased, relative to untreated samples, and comparable to the migration
369 of SMARCAL1 from mock-infected cells (cf lanes 6 and 8 with lane 1, Figure 4A).

370 Treatment with the NAE inhibitor promoted limited phosphorylation of SMARCAL1 (cf
371 lanes 3 and 4, Figure 4A). To determine which SMARCAL1 residues were phosphorylated
372 following Ad infection we immunoprecipitated SMARCAL1 from mock, Ad5 and Ad12 -
373 infected A549 cells and following SDS-PAGE, and gel-slice processing we subjected isolated
374 tryptic peptides to tandem array mass spectrometry (MS/MS). MS analyses revealed that
375 SMARCAL1 was phosphorylated at three major sites following both Ad5 and Ad12
376 infection: S123, S129 and S173 (Figure 4B). S123 and S129 formed part of a minimal CDK
377 consensus phosphorylation motif, SP, whilst S173 formed part of an ATR consensus
378 phosphorylation motif, SQE. Sequence homology searches revealed that these residues were
379 conserved amongst primates, but less well conserved for lower mammals (Figure 4C).

380 **Pharmacological inhibition of ATR kinase and CDK activities limits SMARCAL1**
381 **degradation following Ad5 and Ad12 infection.** Given that SMARCAL1 phosphorylation
382 precedes its degradation following Ad infection we next investigated whether the ATR and
383 CDK -dependent phosphorylation of SMARCAL1 during Ad infection was an essential
384 prerequisite for the Ad-induced degradation of SMARCAL1. To do this we studied the
385 effects of the selective ATR kinase inhibitor, AZD6738, and the CDK inhibitor, RO-3306, on
386 the ability of both *wt* Ad5 and *wt* Ad12 to induce the degradation of SMARCAL1. Initially,
387 therefore, A549 cells were either mock-infected or infected with *wt* Ad5 or *wt* Ad12, and then
388 incubated in the absence or presence of AZD6738 for specific times post-infection. WB
389 analyses revealed that treatment of A549 cells with AZD6738 reduced modestly the ability of
390 *wt* Ad5 to promote the degradation of SMARCAL1 (cf lanes 7 and 8 with lanes 5 and 6,
391 Figure 5A). Interestingly, however, the effect of AZD6738 treatment on the ability of *wt*
392 Ad12 to promote SMARCAL1 degradation was much more dramatic; the ATR kinase
393 inhibitor reduced appreciably the ability of *wt* Ad12 to stimulate SMARCAL1 degradation
394 during infection, with no observable degradation at 24h post-infection (cf lanes 7 and 8 with

lanes 5 and 6, Figure 5B). To establish whether CDKs cooperate with ATR to promote SMARCAL1 degradation following Ad infection we infected A549 cells with either *wt* Ad5, or *wt* Ad12 then incubated infected cells in the absence, or presence, of AZD6738 and RO-3306 for specific times post-infection. WB analyses revealed that the use of both inhibitors reduced substantially the ability of *wt* Ad5 to promote the degradation of SMARCAL1, particularly at 48h post-infection (cf lanes 5 and 6 with lanes 7 and 8, Figure 5C). Similarly, the combined effects of AZD6738 and RO-3306 were to almost abate entirely the ability of *wt* Ad12 to induce the degradation of SMARCAL1 (cf lanes 5 and 6 with lanes 7 and 8, Figure 5D). Taken together these data suggest strongly that the combined ATR kinase and CDK -dependent phosphorylation of SMARCAL1 facilitate the E1B-55K/E4orf6-dependent degradation of SMARCAL1 during Ad infection. As such, these studies are important in establishing that Ad can activate, and then utilise, cellular kinases during infection to promote viral replication.

SMARCAL1 recruitment to VRCs is largely dependent upon its association with the RPA complex but is also regulated by ATR and CDK -dependent phosphorylation. To explore in more detail the factors that modulate the recruitment of SMARCAL1 to VRCs during Ad infection we generated a phosphorylation-defective GFP-SMARCAL1- Δ P (S123A, S129A and S173A) mutant in order to ablate the ATR, and CDK, -dependent phosphorylation of SMARCAL1 in response to Ad infection, and utilised a GFP-SMARCAL1- Δ RPA mutant that is unable to bind the RPA complex (21). We then generated clonal, RPE-1 cell lines that expressed constitutively, either GFP alone, *wt* GFP-SMARCAL1, GFP-SMARCAL1- Δ P or GFP-SMARCAL1- Δ RPA. Then, to investigate the role SMARCAL1 phosphorylation and the RPA complex play in SMARCAL1 recruitment to VRCs we infected these cell lines with either *wt* Ad5 or *wt* Ad12, and analysed GFP-SMARCAL1 cellular distribution throughout the infection process. Pertinently, Ad infection

420 of GFP alone RPE-1 cells had no effect upon the pan-cellular distribution of GFP (data not
421 shown). In mock-infected RPE-1 cells *wt* GFP-SMARCAL1, GFP-SMARCAL1- Δ P and
422 GFP-SMARCAL1- Δ RPA were distributed evenly throughout the nucleus (panels i-iii, Figure
423 6A). Following infection of RPE-1 cells with either *wt* Ad5, or *wt* Ad12, *wt* GFP-
424 SMARCAL1 was re-distributed to VRCs (panels iv and vii respectively, Figure 6A).
425 Interestingly, the ability of both *wt* Ad5 and *wt* Ad12 to promote the recruitment of the GFP-
426 SMARCAL1- Δ P mutant to VRCs, relative to *wt* GFP-SMARCAL1 was reduced
427 significantly, but only by one-third (panels v and viii, Figure 6A; Figure 6B). Moreover, the
428 ability of both *wt* Ad5 and *wt* Ad12 to promote the recruitment of GFP-SMARCAL1- Δ RPA,
429 relative to *wt* GFP-SMARCAL1, was also reduced significantly, by approximately two-thirds
430 (panels vi and ix, Figure 6A; Figure 6B). Taken together, these data suggest that the RPA
431 complex plays a major role in the recruitment of SMARCAL1 to VRCs during Ad infection,
432 whilst the ATR- and CDK- dependent phosphorylation of SMARCAL1, although not
433 essential, also contributes towards SMARCAL1 recruitment to VRCs following Ad infection.

434 Given that ATR and CDK inhibitors restricted the ability of both *wt* Ad5 and *wt* Ad12 to
435 promote SMARCAL1 degradation during infection, we also wished to use this experimental
436 system to explore the specific roles of S123, S129 and S173 phosphorylation in the Ad-
437 mediated degradation of SMARCAL1. Unfortunately, Ad infection of RPE-1 cells that
438 constitutively expressed GFP-SMARCAL1 species resulted in the enhanced expression of
439 GFP-SMARCAL1 species, probably as a result of E1A transactivation of the CMV promoter
440 driving the expression of GFP-SMARCAL1 species (data not shown). As such we were not
441 able to determine the individual contribution of specific SMARCAL1 phosphorylation sites
442 in the Ad-induced degradation process.

443 **Ad5 and Ad12 E1B-55K associate with SMARCAL1 in Ad-transformed cells.** As E1B-
444 55K has previously been shown to function as a substrate adaptor in the recruitment of
445 cellular proteins, such as p53 and MRE11, for CRL-dependent degradation during infection
446 we next investigated whether E1B-55K also served as an adaptor for SMARCAL1 and could
447 be found associated with SMARCAL1 in Ad-transformed cells. To investigate whether Ad5
448 and Ad12 E1B-55K were found associated with SMARCAL1 in Ad-transformed cells we
449 performed reciprocal co-immunoprecipitation studies using Ad5 HEK 293 cells and Ad12
450 HER2 cells. Consistent with the notion that E1B-55K and SMARCAL1 associate *in vivo*,
451 anti-E1B-55K antibodies co-immunoprecipitated SMARCAL1, and anti-SMARCAL1
452 antibodies co-immunoprecipitated E1B-55K, from both Ad5 HEK 293 cells and Ad12 HER2
453 cells (Figure 7A and 7B, respectively). Given that p53 is a known E1B-55K-interacting
454 protein, we performed reciprocal p53 and E1B-55K co-immunoprecipitation studies to
455 validate the approach taken (Figure 7A and 7B, respectively).

456 **Generation of Ad5 and Ad12 E1B-55K FlpIn T-REX U2OS clonal cell lines.** As we have
457 shown that Ad E1B-55K can associate with SMARCAL1 in Ad-transformed cells (Figure 7)
458 we wished to investigate the specific effects of E1B-55K expression, in isolation, upon
459 SMARCAL1 function. To begin to do this we first generated clonal TET-inducible Ad5 and
460 Ad12 E1B-55K FlpIn U2OS cells that upon induction with the tetracycline analogue,
461 doxycycline, expressed Ad5 and Ad12 E1B-55K (Figure 8). Consistent with the role for Ad
462 E1B-55K in the stabilization of the p53 tumour suppressor, p53 protein levels were also
463 increased following both Ad5 and Ad12 E1B-55K (Figure 8). Unlike p53, the protein levels
464 of SMARCAL1 and another E1B-55K binding partner, MRE11, were not altered appreciably,
465 following E1B-55K expression (Figure 8). Taken together, these data demonstrate that we
466 have generated TET-inducible Ad5 and Ad12 E1B-55K FlpIn U2OS cells that express
467 functional E1B-55K following treatment with doxycycline.

468 **Ad5 and Ad12 E1B-55K dysregulate DNA fork speed during cellular DNA replication**
469 **and promote replication fork collapse.** It is well established that in addition to its role as a
470 substrate adaptor in the CRL-dependent degradation of p53 during Ad infection, E1B-55K
471 can, in isolation, also inhibit the transactivation properties of p53 (31). As SMARCAL1
472 possesses the inherent ability to prevent replication fork collapse in unperturbed S-phase and,
473 in response to agents that promote replication stress, promote replication fork restart after
474 fork collapse we wished to establish whether Ad E1B-55K could also modulate the cellular
475 functions of SMARCAL1. To measure the effects of Ad E1B-55K expression upon
476 replication fork speed during unperturbed S-phase we utilised the DNA fibre assay. To do
477 this we pulse-labelled FIPIn U2OS cells (+/- Ad5 or Ad12 E1B-55K expression) successively
478 with the thymidine analogues, CldU and IdU for 20 minutes each to label DNA at replication
479 forks. DNA fibre analyses revealed that in the presence of Ad5 E1B-55K, or Ad12 E1B-55K
480 CldU-labelled tracks of newly synthesized DNA were significantly longer, relative to mock
481 controls, suggesting that both Ad5, and Ad12 E1B-55K expression led specifically to
482 accelerated speeds of replication fork progression (Figures 9 A and B). Interestingly however,
483 this accelerated fork speed at on-going DNA replication forks, in the presence of Ad E1B-
484 55K, was not maintained when cells were subsequently labelled with IdU, such that IdU track
485 length was comparable to cells that did not express Ad E1B-55K (Figures 9 A and B). As an
486 increased CldU/IdU ratio can be indicative of fork stalling or collapse (32) we next quantified
487 the effects of Ad E1B-55K expression on replication fork collapse. Consistent with the notion
488 that the Ad E1B-55K-dependent acceleration in fork speed results in replication fork
489 collapse, cells that expressed either Ad5 or Ad12 E1B-55K had a significantly increased
490 number of stalled replication forks (CldU-only labelled DNA fibres) relative to cells that do
491 not express Ad E1B-55K (Figure 9C). Taken together, these data indicate that Ad E1B-55K,
492 can in isolation, modulate cellular DNA replication, and in consideration of the known

493 functions of SMARCAL1, is supportive of the notion that Ad E1B-55K interaction with
494 SMARCAL1 contributes towards dysregulated cellular DNA replication.

495 **Discussion**

496 It is now well established that Ad engages with cellular CRLs to stimulate the ubiquitin-
497 mediated degradation of a small number of cellular DDR proteins in order to promote viral
498 replication (1, 2). Typically, E4orf6, serves to recruit CRLs to protein substrates through
499 direct interaction with CRL components Elongin B and Elongin C, whilst E1B-55K through
500 direct interaction with both E4orf6 and protein substrates, recruits cellular proteins to CRLs
501 for polyubiquitylation and proteasome-mediated degradation (1, 2). Using well-established
502 Ad5 and Ad12 mutant viruses we show that Ad likely utilizes this canonical pathway to
503 promote the degradation of the cellular replication protein, SMARCAL1, during infection
504 (Figures 2 and 3). Indeed, treatment with the NAE inhibitor reduced the extent of degradation
505 of SMARCAL1 during infection, suggesting that CRLs contribute to this degradation
506 process.

507 It was evident during our studies that, prior to its degradation, a higher molecular weight
508 form of SMARCAL1 was observed upon SDS-PAGE (Figure 2). In this regard we used mass
509 spectrometry to establish that SMARCAL1 was phosphorylated on residues S123, S129 and
510 S173 early during both Ad5 and Ad12 infection (Figure 4). S123 and S129 form part of
511 minimal CDK consensus SP motifs and S173, forms part of a consensus ATM/ATR SQE
512 motif. Although all of these residues have been shown previously to be phosphorylated *in*
513 *vivo* the biological significance of these phosphorylation events has yet to be determined (28).
514 Given that S123 and S129 are likely to be phosphorylated by a CDK and S173 is likely
515 phosphorylated by ATR we investigated whether small molecule inhibitors of ATR kinase
516 and CDKs could affect the ability of Ad to promote SMARCAL1 degradation. Significantly,

517 studies with the ATR inhibitor, AZD6738 and CDK inhibitor, RO-3306, determined that
518 ATR and CDKs cooperate to promote the Ad-targeted degradation of SMARCAL1 during
519 infection (Figure 5), suggesting that S123, S129 and S173 all contribute towards
520 SMARCAL1 stability *in vivo*. Although RO-3306 has greater selectivity for CDK1 than
521 CDK2 and CDK4 (33) Ad infection is known to stimulate the activity of all three kinases
522 (34), such that we cannot, at present, state which CDK(s) is/are responsible for
523 phosphorylating SMARCAL1 during Ad infection. We wished to investigate further the role
524 of phosphorylation of these specific residues in the Ad-mediated degradation of
525 SMARCAL1. To this end we made GFP-SMARCAL1 RPE-1 cell lines where S123, S129
526 and S173 residues were all mutated to A to ablate phosphorylation at these sites. Although we
527 were able to generate clonal cell lines that expressed these mutations, we were unable to
528 undertake these studies as Ad infection results in the transactivation of the CMV promoter
529 that regulates GFP-SMARCAL1 expression (data not shown).

530 We were however, able to use the *wt* GFP-SMARCAL1 and GFP-SMARCAL1 phospho-
531 mutant RPE-1 cell lines to address the role of SMARCAL1 phosphorylation in the
532 recruitment of SMARCAL1 to VRCs. As such, we determined that ATR and CDKs, although
533 not essential, contributed to some extent in the recruitment of SMARCAL1 to VRCs during
534 infection (Figure 6). Moreover, using a GFP-SMARCAL1 species lacking its N-terminal
535 RPA interaction motif we were also able to establish that SMARCAL1 association with RPA
536 is a major determinant in SMARCAL1 recruitment to VRCs (Figure 6). SMARCAL1 was
537 initially characterized as an RPA-interacting protein, and its recruitment to replication forks
538 and sites of DNA damage was shown to be dependent upon its interaction with RPA (21-25).
539 More recent studies have determined that RPA in addition to its ability to control
540 SMARCAL1 localization also confers substrate specificity and regulates SMARCAL1 fork-
541 remodelling reactions through the orientation of its high affinity DNA-binding domains (35).

542 RPA is a single-stranded DNA binding protein complex that has long been known to promote
543 large T-antigen-dependent SV40 DNA replication (36). Although RPA has been shown to be
544 recruited to Ad VRCs during infection its precise role in Ad replication is not known (19, 20).
545 Given that SMARCAL1 is an RPA-binding protein and that most of its activities are
546 controlled by RPA, it is interesting to speculate that any pro-viral RPA functions during Ad
547 infection are not coordinated through the activation of SMARCAL1-dependent remodelling
548 activities. Indeed, as SMARCAL1 is degraded during infection (Figure 2), it is highly likely
549 that SMARCAL1 possesses anti-viral activities. As the mechanism of SV40 DNA replication
550 is well established it would be interesting to determine the requirement for SMARCAL1 in
551 RPA-dependent SV40 DNA replication.

552 Given the role of SMARCAL1 in cellular DNA replication we investigated the effects of Ad
553 E1B-55K expression on cellular DNA replication. We observed that E1B-55K expression
554 enhanced nascent cellular DNA replication fork speed but, ultimately, E1B-55K expression
555 resulted in increased replication fork stalling (Figure 9). It has been determined previously
556 that loss of SMARCAL1 prevents replication re-start after replication stress, resulting in
557 stalled replication, whilst knockdown of p53 and MRE11, also promote stalled cellular DNA
558 replication (28, 37, 38). More generally, it has been determined that oncogene product
559 expression can enhance replication stress to either increase, or decrease, DNA replication
560 initiation, elongation, fork speed, fork stalling and fork re-start through the modulation of
561 origin firing, replication-transcription collisions, reactive oxygen species, and defective
562 nucleotide metabolism (39). It is plausible therefore that the E1B-55K oncoprotein promotes
563 replication stress in Ad-infected cells through interaction with p53, MRE11, SMARCAL1
564 and potentially other cellular targets that ultimately results in cellular DNA replication
565 inhibition. Given the known role of E1B-55K in the promotion of late viral mRNA
566 accumulation and the inhibition of cellular mRNA transport, and translation, in the mediation

567 of host protein shutoff, as well as the proposed role for Ad-mediated protein degradation in
568 mRNA export (40, 41) we postulate that E1B-55K similarly inhibits cellular DNA replication
569 and promotes viral replication through the specific targeting of cellular E1B-55K-interacting
570 proteins for degradation during infection.

571 **Acknowledgements**

572 We would like to thank David Cortez (Vanderbilt University, Nashville, TN) for
573 SMARCAL1 reagents and Thomas Dobner (Heinrich Pette Institute, Hamburg, Germany) for
574 adenovirus 5 mutants. We would also like to thank the BBSRC MIBTP programme for
575 funding for Maria Teresa Tilotta and Simon Davis (BB/M01116X/1; BB/J014532/1) and
576 Jazan and Taibah Universities, Saudi Arabia, for funding Fadi Qashqari and Abeer Albalawi,
577 respectively.

578

579 **References**

- 580 1. Turnell AS, Grand RJ. 2012. Viral regulation of DNA damage response pathways. *J.*
581 *Gen. Virol.* **93**:2076-2097. doi:10.1099/vir.0.044412-0.
- 582 2. Weitzman MD, Fradet-Turcotte A. 2018. Virus DNA replication and the Host DNA
583 Damage Response. *Annual Review of Virology* **5**:141-164.
- 584 3. Dybas JM, Herrmann C, Weitzman MD. 2018. Ubiquitination at the interface of
585 tumor viruses and DNA damage responses. *Curr Opin Virol.* **32**:40-47. doi:
586 10.1016/j.coviro.2018.08.017.
- 587 4. Querido E, Blanchette P, Yan Q, Kamura T, Morrison M, Boivin D, Kaelin WG,
588 Conaway RC, Conaway JW, Branton PE. 2001. Degradation of p53 by adenovirus
589 E4orf6 and E1B55K proteins occurs via a novel mechanism involving a cullin-
590 containing complex. *Genes Dev* **15**:3104-3117. doi:10.1101/gad.926401.

- 591 5. Harada JN, Shevchenko A, Shevchenko A, Pallas DC, Berk AJ. 2002. Analysis of the
592 adenovirus E1B-55K-anchored proteome reveals its link to ubiquitination machinery.
593 *J Virol.* **6**:9194-9206.
- 594 6. Blanchette P, Cheng CY, Yan Q, Ketner G, Ornelles DA, Dobner T, Conaway RC,
595 Conaway JW, Branton PE. 2004. Both BC-box motifs of adenovirus protein E4orf6
596 are required to efficiently assemble an E3 ligase complex that degrades p53. *Mol Cell*
597 *Biol.* **24**:9619-9629.
- 598 7. Blackford AN, Patel RN, Forrester NA, Theil K, Groitl P, Stewart GS, Taylor AMR,
599 Morgan IM, Dobner T, Grand RJA, Turnell AS. 2010. Adenovirus 12 E4orf6 inhibits
600 ATR activation by promoting TOPBP1 degradation. *Proc. Natl. Acad. Sci. USA.*
601 **107**:12251-12256. doi:10.1073/pnas.0914605107.
- 602 8. Cheng CY, Gilson T, Wimmer P, Schreiner S, Ketner G, Dobner T, Branton PE,
603 Blanchette P. 2013. Role of E1B55K in E4orf6/E1B55K E3 ligase complexes formed
604 by different human adenovirus serotypes. *J Virol.* **87**:6232-45. doi:
605 10.1128/JVI.00384-13.
- 606 9. Stracker TH, Carson CT, Weitzman MD. 2002. Adenovirus oncoproteins inactivate
607 the MRE11-Rad50-NBS1 DNA repair complex. *Nature* **418**:348-352.
608 doi:10.1038/nature00863.
- 609 10. Orazio NI, Naeger CM, Karlseder J, Weitzman MD. 2011. The adenovirus
610 E1b55K/E4orf6 complex induces degradation of the Bloom helicase during infection.
611 *J Virol* **85**:1887-1892. doi:10.1128/JVI.02134-10.
- 612 11. Baker A, Rohleder KJ, Hanakahi LA, Ketner G. 2007. Adenovirus E4 34k and E1b
613 55k oncoproteins target host DNA ligase IV for proteasomal degradation. *J Virol*
614 **81**:7034-7040. doi:10.1128/JVI.00029-07.

- 615 12. Dallaire F, Blanchette P, Groitl P, Dobner T, Branton PE. 2009. Identification of
616 integrin $\alpha 3$ as a new substrate of the adenovirus E4orf6/E1B 55-kilodalton E3
617 ubiquitin ligase complex. *J Virol* **83**:5329–5338. doi:10.1128/JVI.00089-09.
- 618 13. Fu YR, Turnell AS, Davis S, Heesom KJ, Evans VC, Matthews DA. 2017.
619 Comparison of protein expression during wild-type, and E1B-55k-deletion,
620 adenovirus infection using quantitative time-course proteomics. *J Gen Virol*. **98**:1377-
621 1388. doi: 10.1099/jgv.0.000781.
- 622 14. Schreiner S, Wimmer P, Groitl P, Chen SY, Blanchette P, Branton PE, Dobner T.
623 2011. Adenovirus type 5 early region 1B 55K oncoprotein-dependent degradation of
624 cellular factor Daxx is required for efficient transformation of primary rodent cells. *J*
625 *Virol* **85**:8752–8765. doi:10.1128/JVI.00440-11.
- 626 15. Forrester NA, Patel RN, Speiseder T, Groitl P, Sedgwick GG, Shimwell NJ, Seed RI,
627 Catnagh PÓ, McCabe CJ, Stewart GS, Dobner T, Grand RJ, Martin A, Turnell AS.
628 2012. Adenovirus E4orf3 targets transcriptional intermediary factor 1γ for
629 proteasome-dependent degradation during infection. *J Virol* **86**:3167–3179.
630 doi:10.1128/JVI.06583-11.
- 631 16. Sohn SY, Hearing P. 2016. The adenovirus E4-ORF3 protein functions as a SUMO
632 E3 ligase for TIF- 1γ sumoylation and poly-SUMO chain elongation. *Proc Natl Acad*
633 *Sci U S A*. **113**:6725-6730. doi: 10.1073/pnas.1603872113.
- 634 17. Bridges RG, Sohn SY, Wright J, Leppard KN, Hearing P. 2016. The Adenovirus E4-
635 ORF3 Protein Stimulates SUMOylation of General Transcription Factor TFII-I to
636 Direct Proteasomal Degradation. *MBio*. **7**:e02184-15. doi: 10.1128/mBio.02184-15.
- 637 18. Blackford AN, Jackson SP. 2017. ATM, ATR, and DNA-PK: the trinity at the heart
638 of the DNA damage response. *Mol Cell* **66**:801–817.
639 doi:10.1016/j.molcel.2017.05.015.

- 640 19. Carson CT, Orazio NI, Lee DV, Suh J, Bekker-Jensen S, Araujo FD, Lakdawala SS,
641 Lilley CE, Bartek J, Lukas J, Weitzman MD. 2009. Mislocalization of the MRN
642 complex prevents ATR signaling during adenovirus infection. *EMBO J* **28**:652–662.
643 doi:10.1038/emboj.2009.15.
- 644 20. Blackford AN, Bruton RK, Dirlik O, Stewart GS, Taylor AM, Dobner T, Grand RJ,
645 Turnell AS. 2008. A role for E1B-AP5 in ATR signaling pathways during adenovirus
646 infection. *J Virol* **82**:7640–7652. doi:10.1128/JVI.00170-08.
- 647 21. Bansbach CE, Bétous R, Lovejoy CA, Glick GG, Cortez D. 2009. The annealing
648 helicase SMARCAL1 maintains genome integrity at stalled replication forks. *Genes*
649 *Dev.* **23**:2405-2414. doi: 10.1101/gad.1839909.
- 650 22. Ciccia A, Bredemeyer AL, Sowa ME, Terret ME, Jallepalli PV, Harper JW, Elledge
651 SJ. 2009. The SIOD disorder protein SMARCAL1 is an RPA-interacting protein
652 involved in replication fork restart. *Genes Dev.* **23**:2415-2425. doi:
653 10.1101/gad.1832309.
- 654 23. Postow L, Woo EM, Chait BT, Funabiki H. 2009. Identification of SMARCAL1 as a
655 component of the DNA damage response. *J Biol Chem.* 284:35951-35961. doi:
656 10.1074/jbc.M109.048330.
- 657 24. Yusufzai T, Kong X, Yokomori K, Kadonaga JT. 2009. The annealing helicase
658 HARP is recruited to DNA repair sites via an interaction with RPA. *Genes Dev.*
659 **23**:2400–2404.
- 660 25. Yuan J, Ghosal G, Chen J. 2009. The annealing helicase HARP protects stalled
661 replication forks. *Genes Dev.* **23**:2394–2399.
- 662 26. Boerkoel CF, Takashima H, John J, Yan J, Stankiewicz P, Rosenbarker L, André JL,
663 Bogdanovic R, Burguet A, Cockfield S, Cordeiro I, Fründ S, Illies F, Joseph M,
664 Kaitila I, Lama G, Loirat C, McLeod DR, Milford DV, Petty EM, Rodrigo F, Saraiva

- 665 JM, Schmidt B, Smith GC, Spranger J, Stein A, Thiele H, Tizard J, Weksberg R,
666 Lupski JR, Stockton DW. 2002. Mutant chromatin remodeling protein SMARCAL1
667 causes Schimke immuno-osseous dysplasia. *Nat Genet.* **30**:215-220.
- 668 27. Carroll C, Bansbach CE, Zhao R, Jung SY, Qin J, Cortez D. 2014. Phosphorylation of
669 a C-terminal auto-inhibitory domain increases SMARCAL1 activity. *Nucleic Acids*
670 *Res.* **42**:918-925. doi: 10.1093/nar/gkt929.
- 671 28. Couch FB, Bansbach CE, Driscoll R, Luzwick JW, Glick GG, Bétous R, Carroll CM,
672 Jung SY, Qin J, Cimprich KA, Cortez D. 2013. ATR phosphorylates SMARCAL1 to
673 prevent replication fork collapse. *Genes Dev.* **27**:1610-1623. doi:
674 10.1101/gad.214080.113.
- 675 29. Soucy TA, Smith PG, Milhollen MA, Berger AJ, Gavin JM, Adhikari S, Brownell JE,
676 Burke KE, Cardin DP, Critchley S, Cullis CA, Doucette A, Garnsey JJ, Gaulin JL,
677 Gershman RE, Lublinsky AR, McDonald A, Mizutani H, Narayanan U, Olhava EJ,
678 Peluso S, Rezaei M, Sintchak MD, Talreja T, Thomas MP, Traore T, Vyskocil S,
679 Weatherhead GS, Yu J, Zhang J, Dick LR, Claiborne CF, Rolfe M, Bolen JB,
680 Langston SP. 2009. An inhibitor of NEDD8-activating enzyme as a new approach to
681 treat cancer. 458:732-736. doi: 10.1038/nature07884.
- 682 30. Bailly A, Perrin A, Bou Malhab LJ, Pion E, Larance M, Nagala M, Smith P,
683 O'Donohue MF, Gleizes PE, Zomerdijk J, Lamond AI, Xirodimas DP. 2016. The
684 NEDD8 inhibitor MLN4924 increases the size of the nucleolus and activates p53
685 through the ribosomal-Mdm2 pathway. *Oncogene* **35**:415-426. doi:
686 10.1038/onc.2015.104.
- 687 31. Yew, PR, Berk AJ. 1992. Inhibition of p53 transactivation required for transformation
688 by adenovirus early 1B protein. *Nature* **357**:82-85.

- 689 32. Petermann E, Maya-Mendoza A, Zachos G, Gillespie DAF, Jackson DA, Caldecott
690 KW. 2006. Chk1 Requirement for High Global Rates of Replication Fork Progression
691 during Normal Vertebrate S Phase. *Mol. Cell. Biol.* **26**: 3319-3326.
692 doi:10.1128/MCB.26.8.3319-3326.2006
- 693 33. Vassilev LT, Tovar C, Chen S, Knezevic D, Zhao X, Sun H, Heimbros DC, Chen L.
694 2006. Selective small-molecule inhibitor reveals critical mitotic functions of human
695 CDK1. *Proc Natl Acad Sci U S A.* 103:10660-10665. doi: 10.1073/pnas.0600447103.
- 696 34. Grand RJ, Ibrahim AP, Taylor AMR, Milner AE, Gregory CD, Gallimore PH, Turnell
697 AS. 1998. Human cells arrest in S phase in response to adenovirus 12 E1A. *Virology*
698 **244**:330-342.
- 699 35. Bhat KP, Bétous R, Cortez D. 2015. High-affinity DNA-binding domains of
700 replication protein A (RPA) direct SMARCAL1-dependent replication fork
701 remodeling. *J Biol Chem.* **290**:4110-4117. doi: 10.1074/jbc.M114.627083.
- 702 36. Wold MS, Kelly T. 1988. Purification and characterization of replication protein A, a
703 cellular protein required for in vitro replication of simian virus 40 DNA. *Proc Natl*
704 *Acad Sci U S A.* **85**:2523-2527.
- 705 37. Klusmann I, Rodewald S, Müller L, Friedrich M, Wienken M, Li Y, Schulz-
706 Heddergott R, Dobbelstein M. 2016. p53 activity results in DNA replication fork
707 processivity. *Cell Rep.* **17**:1845-1857. doi: 10.1016/j.celrep.2016.10.036.
- 708 38. Bryant HE, Petermann E, Schultz N, Jemth AS, Loseva O, Issaeva N, Johansson F,
709 Fernandez S, McGlynn P, Helleday T. 2009. PARP is activated at stalled forks to
710 mediate MRE11-dependent replication restart and recombination. *EMBO J.* **28**:2601-
711 2615. doi: 10.1038/emboj.2009.206.

- 712 39. Kotsantis P, Petermann E, Boulton SJ. 2018. Mechanisms of Oncogene-Induced
713 Replication Stress: Jigsaw Falling into Place. *Cancer Discov.* **8**:537-555. doi:
714 10.1158/2159-8290.CD-17-1461.
- 715 40. Babiss LE, Ginsberg HS, Darnell Jr JE. Adenovirus E1B proteins are required for
716 accumulation of late viral mRNA and for effects on cellular mRNA translation and
717 transport. *Mol. Cell. Biol.* **5** (1985), pp. 2552-2558.
- 718 41. Blanchette P, Kindsmuller K, Groitl P, Dallaire F, Speiseder T, Branton PE, Dobner
719 T. 2008. Control of mRNA export by adenovirus E4orf6 and E1B55K proteins during
720 productive infection requires E4orf6 ubiquitin ligase activity. *J Virol.* **82**: 2642-2651.
721 doi: 10.1128/JVI.02309-07.

722

723

724 **Figure Legends.**

725 **FIG 1.** SMARCAL1 is reorganized to viral replication centres during the early stages of Ad
726 infection. A549 cells were either mock-infected (panels i-iii), or infected with 10 pfu/cell of
727 wt Ad5 (panels iv-vi) or wt Ad12 (panels vii-ix). At 18h post-infection, cells were fixed,
728 permeabilized and co-stained for SMARCAL1 and RPA2. Arrows indicate regions of
729 RPA2/SMARCAL1 co-localization. In all instances images were recorded using a Zeiss
730 LSM510-Meta confocal microscope.

731 **FIG 2.** SMARCAL1 is targeted for degradation during Ad infection. A549 cells were either
732 mock-infected or infected with 10 pfu/cell of wt Ad5 or wt Ad12 and harvested at the
733 appropriate times post-infection. (A) Ad5 cell lysates were then subject to WB for
734 SMARCAL1, p53, E1B-55K, E4orf6 and β -actin. (B) Ad12 cell lysates were subject to WB
735 for SMARCAL1, p53, E1B-55K and β -actin. h.p.i - hours post-infection. Representative of
736 more than three independent experiments.

737 **FIG 3.** SMARCAL1 is degraded during Ad infection in an E1B-55K/E4orf6- and CRL-
738 dependent manner. (A) A549 cells were either mock-infected, infected with *wt* Ad5, or
739 infected with E1B-55K (*dl1520*), E4orf3 (*H5pm4150*) or E4orf6 (*H5pm4154*) deletion
740 viruses. At 24 h and 48 h post-infection cells were harvested and subject to WB for
741 SMARCAL1, p53, E1B-55K, E4orf3, E4orf6 and β -actin. (B) A549 cells were either mock-
742 infected, infected with *wt* Ad12, or infected with the E1B-55K (*dl620*) deletion virus. At 24 h
743 and 48 h post-infection cells were harvested and Western blotted for SMARCAL1, p53, E1B-
744 55K, and β -actin. (C and D) A549 cells were either mock-infected or infected with *wt* Ad5 or
745 *wt* Ad12, in the absence or presence of 100 nM or 500 nM MLN4924. At 24 h and 48 h post-
746 infection cells were harvested and subject to WB for SMARCAL1, p53, E1B-55K and β -
747 actin. h.p.i - hours post-infection. Representative of three independent experiments.

748 **FIG 4.** SMARCAL1 is phosphorylated during the early stages of Ad infection. (A) A549
749 cells were either mock-infected, treated with MLN4924, or infected with 10 pfu/cell of *wt*
750 Ad5 or *wt* Ad12 and harvested at 18 h post-infection. Cells were harvested in IP buffer and
751 subject to immunoprecipitation for SMARCAL1. Anti-SMARCAL1 immunoprecipitates
752 collected on protein G-sepharose were treated in the absence, or presence, of λ -phosphatase
753 and then subject to SDS-PAGE and WB for SMARCAL1. (B) SMARCAL1 was
754 immunoprecipitated from mock-infected and *wt* Ad5 or *wt* Ad12 infected A549 cells 18 h
755 post-infection, and separated by SDS-PAGE. Protein bands excised from the gel were subject
756 to trypsinization and mass spectrometric analysis. Identified SMARCAL1 phosphorylated
757 peptides from Ad-infected cells are presented. (C) S123, S129 and S173 are conserved
758 between primates but less well conserved in lower mammals. SMARCAL1 primary
759 sequences from a number of species were aligned using CLUSTAL Omega. Shaded areas
760 indicate conserved residues.

761 **FIG 5.** ATR kinase and CDKs promote SMARCAL1 degradation following Ad5 and Ad12
762 infection. A549 cells were either mock-infected or infected with 10 pfu/cell of *wt* Ad5 (A and
763 C) or *wt* Ad12 (B and D). Cells were then incubated in the absence or presence of ATR
764 inhibitor (AZD6738 (ATRi), 1 μ M; A and B) or ATR and CDK inhibitors (AZD6738, 1 μ M
765 and RO-3306 (CDKi), 9 μ M; C and D) and harvested at the appropriate times post-infection.
766 Cell lysates were then separated by SDS-PAGE and subject to WB for SMARCAL1, p53,
767 E1B-55K, and β -actin. h.p.i - hours post-infection. Representative of three independent
768 experiments.

769 **FIG 6.** SMARCAL1 is recruited to VRCs in an RPA-dependent, and ATR and CDK -
770 dependent, manner. (A) Microscopic images depicting the cellular localization of *wt* GFP-
771 SMARCAL1, GFP-SMARCAL1- Δ P and GFP-SMARCAL1- Δ RPA in mock-infected (panels
772 i-iii), *wt* Ad5-infected (panels iv-vi) or *wt* Ad12-infected cells (panels vii-ix) 18 h post-
773 infection. (B) Bar graph (+/- S.E.M.) showing the % of GFP-labelled cells that are recruited
774 to VRCs following Ad5 or Ad12 infection. n=3 (300 cells per experiment; 900 cells in total).
775 Only those cells that exhibited clear GFP-SMARCAL1 structures in Ad-infected cells,
776 comparable to the known architecture of VRCs at different stages of infection, were counted
777 as VRC positive. Data presented was subjected to ANOVA two-tailed t-test. Significance
778 testing for difference in recruitment of GFP-SMARCAL1- Δ P to VRCs relative to *wt* GFP-
779 SMARCAL1 following Ad5 infection: p = 0.0065 (**); difference in recruitment of GFP-
780 SMARCAL1- Δ RPA to VRCs relative to *wt* GFP-SMARCAL1 following Ad5 infection: p =
781 8.8E-05 (****); difference in recruitment of GFP-SMARCAL1- Δ P to VRCs relative to *wt*
782 GFP-SMARCAL1 following Ad12 infection: p = 0.04 (*); difference in recruitment of GFP-
783 SMARCAL1- Δ RPA to VRCs relative to *wt* GFP-SMARCAL1 following Ad5 infection: p =
784 0.002 (***).

785 **FIG 7.** Ad E1B-55K associates with SMARCAL1 in Ad-transformed cells. (A) Ad E1B-55K
786 and SMARCAL1 were immunoprecipitated from Ad5 HEK 293 cells (A) and Ad12 HER2
787 cells (B) and subject to WB for E1B-55K and SMARCAL1. IgG, immunoglobulin control IP.

788 **FIG 8.** Generation and characterization of TET-inducible Ad5 and Ad12 E1B-55K FlpIn
789 U2OS cells. FlpIn U2OS cells were transfected with Ad5 E1B-55K and Ad12 E1B-55K
790 pcDNA5/FRT/TO plasmids and the recombination plasmid, pOG44. Cells were incubated in
791 selection medium containing hygromycin (200 µg/ml). Individual colonies were isolated,
792 expanded and treated with 0.1 µg/ml doxycycline. 24 h post-induction cell lysates were
793 harvested, separated by SDS-PAGE and subject to WB analysis for Ad5 and Ad12 E1B-55K.
794 WB analyses were also performed to gauge the levels of SMARCAL1, p53, MRE11 and β-
795 actin for Ad5 E1B-55K, and Ad12 E1B-55K, FlpIn U2OS cells, respectively. Representative
796 of more than three independent experiments.

797 **FIG 9.** Ad5 and Ad12 E1B-55K modulate cellular DNA replication rates and promote
798 replication fork stalling. Uninduced, and doxycycline-induced, Ad5 and Ad12 E1B-55K
799 FlpIn U2OS cells were labelled with 25 µM CldU and 250 µM IdU for 20 min each. DNA
800 fibre spreads were then prepared and denatured with 2.5 M HCl. DNA fibres were labelled
801 with the appropriate primary and secondary antibodies and visualised using a Nikon E600
802 microscope. (A and B) Representative DNA spreads (+/- Ad5 or Ad12 E1B-55K) are shown
803 indicating the mean fork speeds; CldU and IdU fork lengths were quantified and presented as
804 dot plots (+/- S.D.) with the mean fork speed shown as a red bar. n = 3 (Total fibres analysed:
805 Ad5 mock = 347; + Ad5 E1B-55K = 368; Ad12 mock = 370; + Ad12 E1B-55K = 364). (C)
806 % stalled forks (CldU-only labelled forks) were quantified and presented as a bar chart +/-
807 S.D. In all instances data presented was subjected to ANOVA two-tailed t-test; + Ad5 E1B-
808 55K CldU tract length relative to mock CldU tract length, p = 4.8E-20 (***) ; + Ad5 E1B-
809 55K CldU/IdU ratio relative to mock CldU tract length, p= 9.44E-45 (****); + Ad12 E1B-

810 55K CldU tract length relative to mock CldU tract length, $p = 1.29E-32$ (****); + Ad12 E1B-
811 55K CldU/IdU ratio relative to mock CldU tract length, $p = 6.32E-61$ (****); ns = not
812 significant. Stalled forks: Ad5 E1B-55K relative to mock, $p = 0.009$ (**); Ad12 E1B-55K
813 relative to mock, $p = 0.002$ (**).

814

815

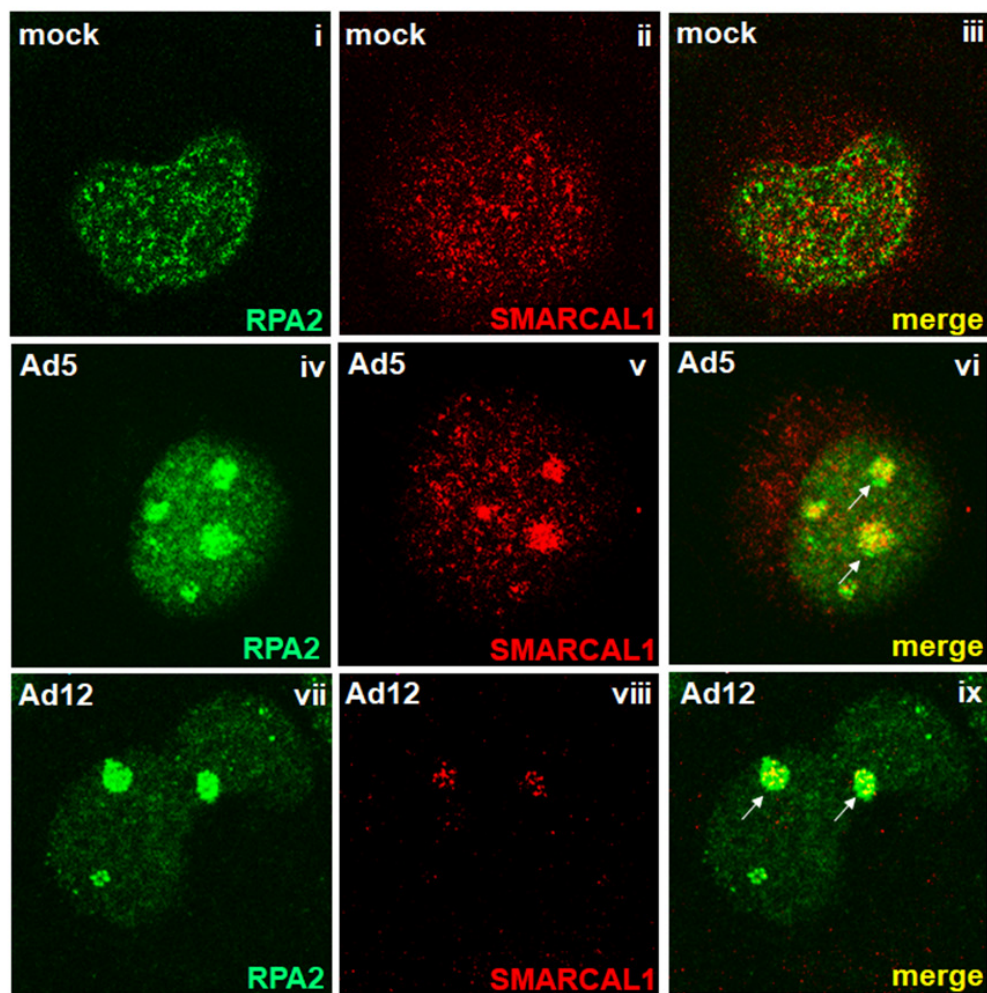


Figure 1

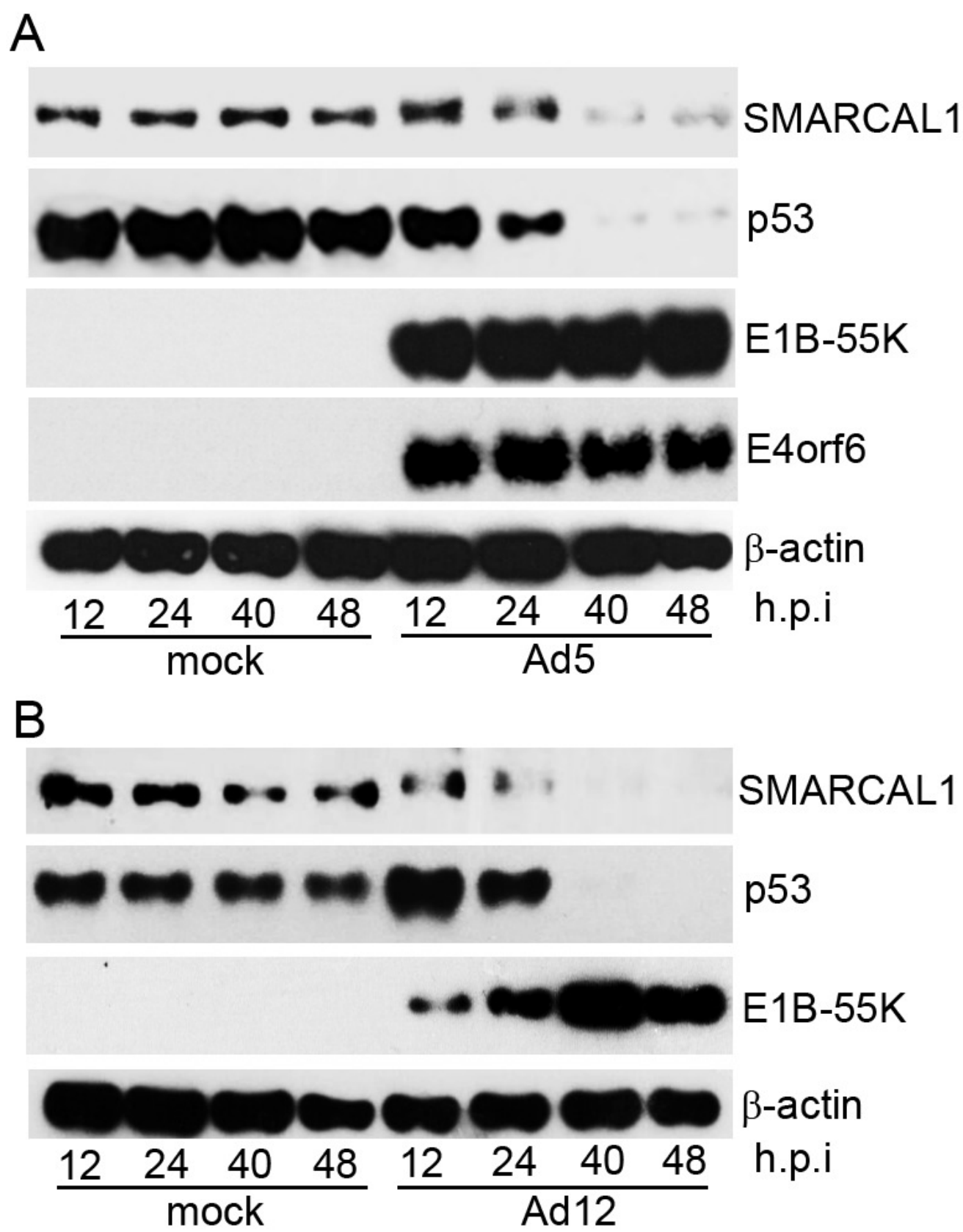


Figure 2

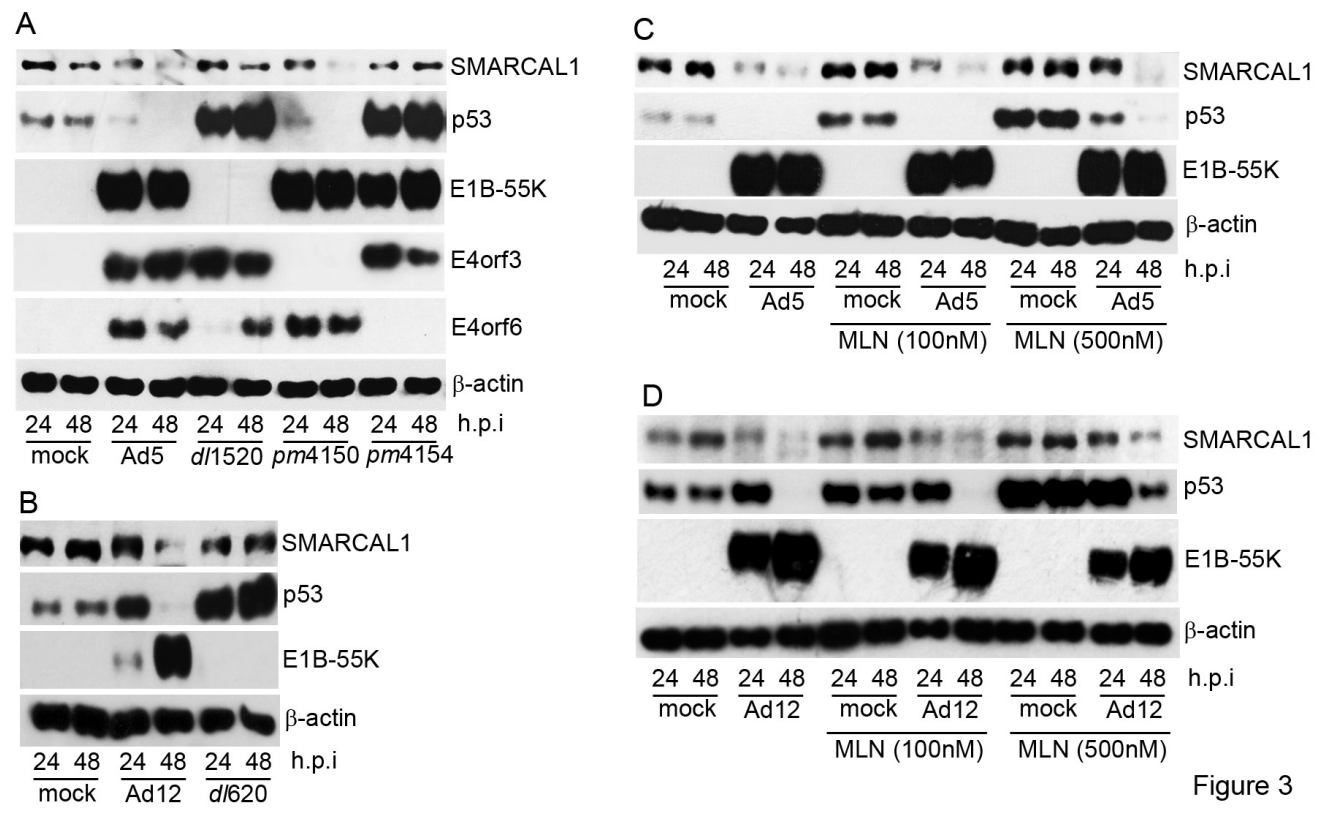


Figure 3

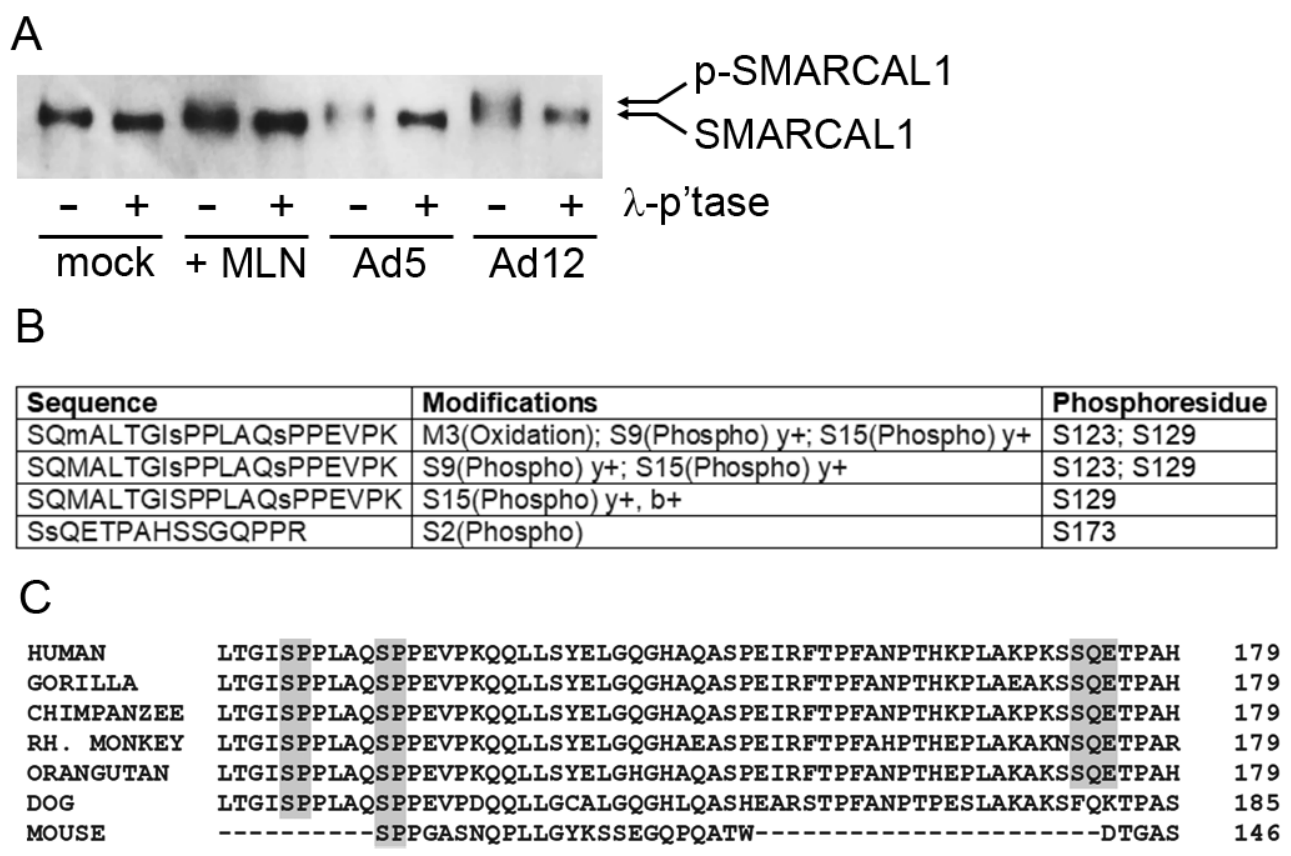


Figure 4

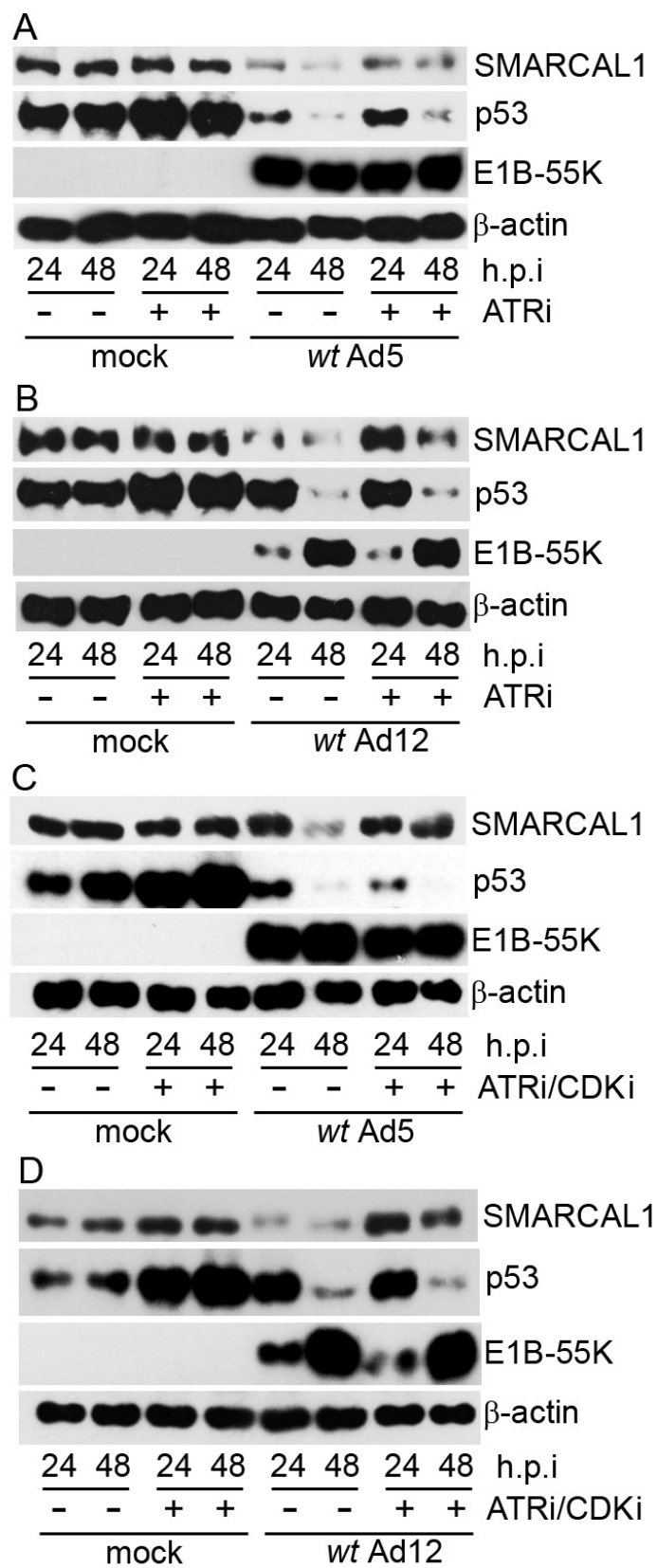


Figure 5

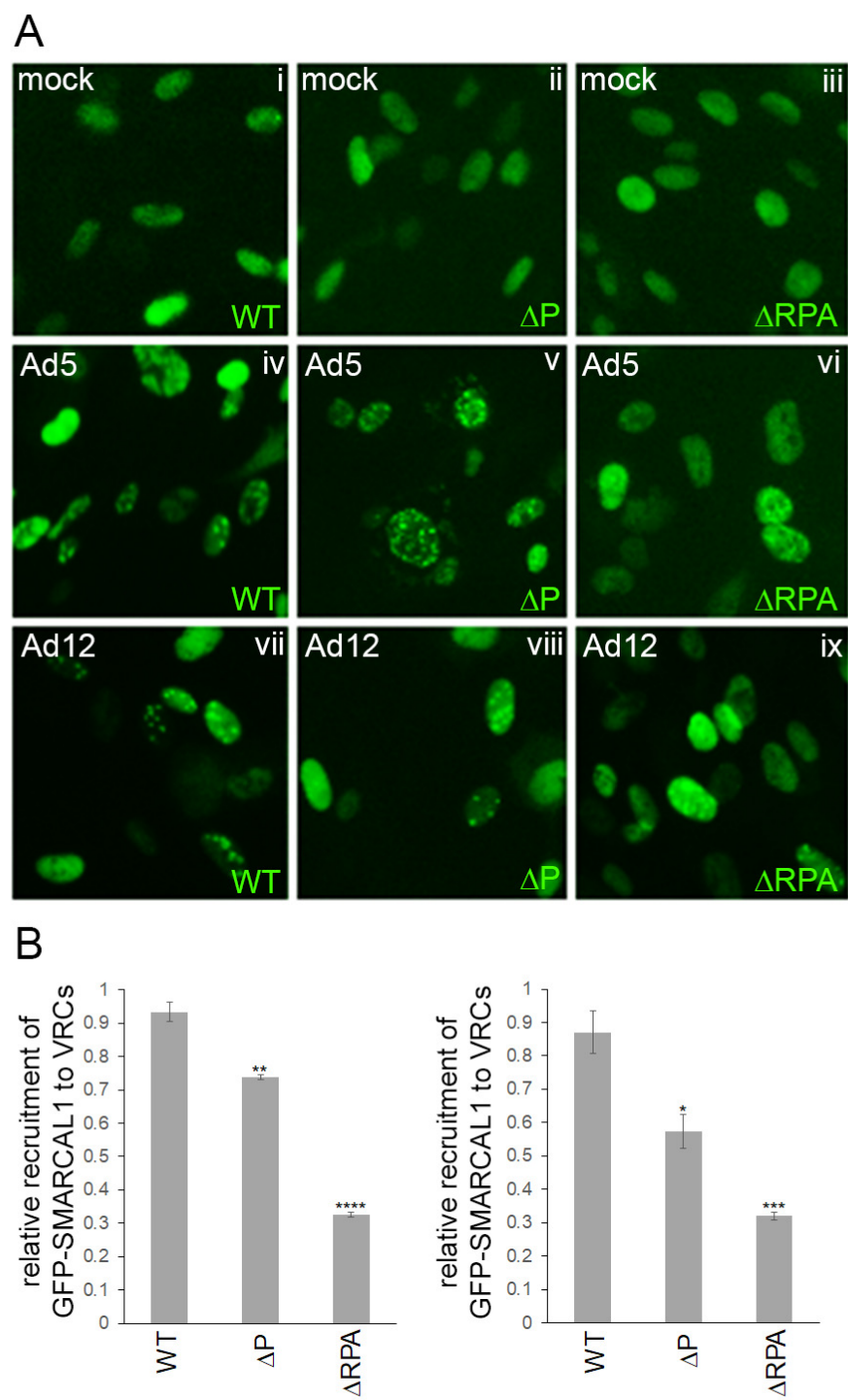


Figure 6

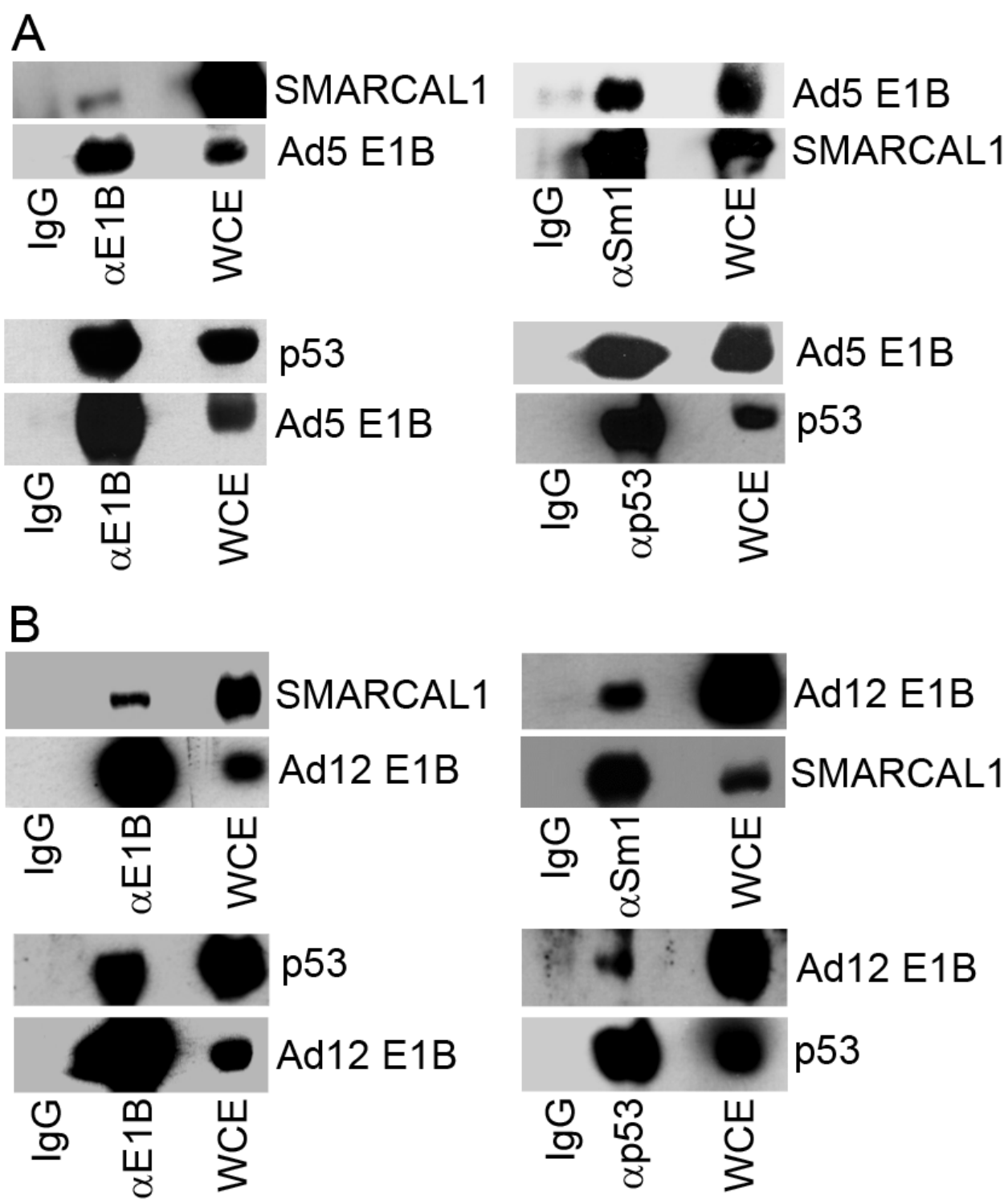


Figure 7

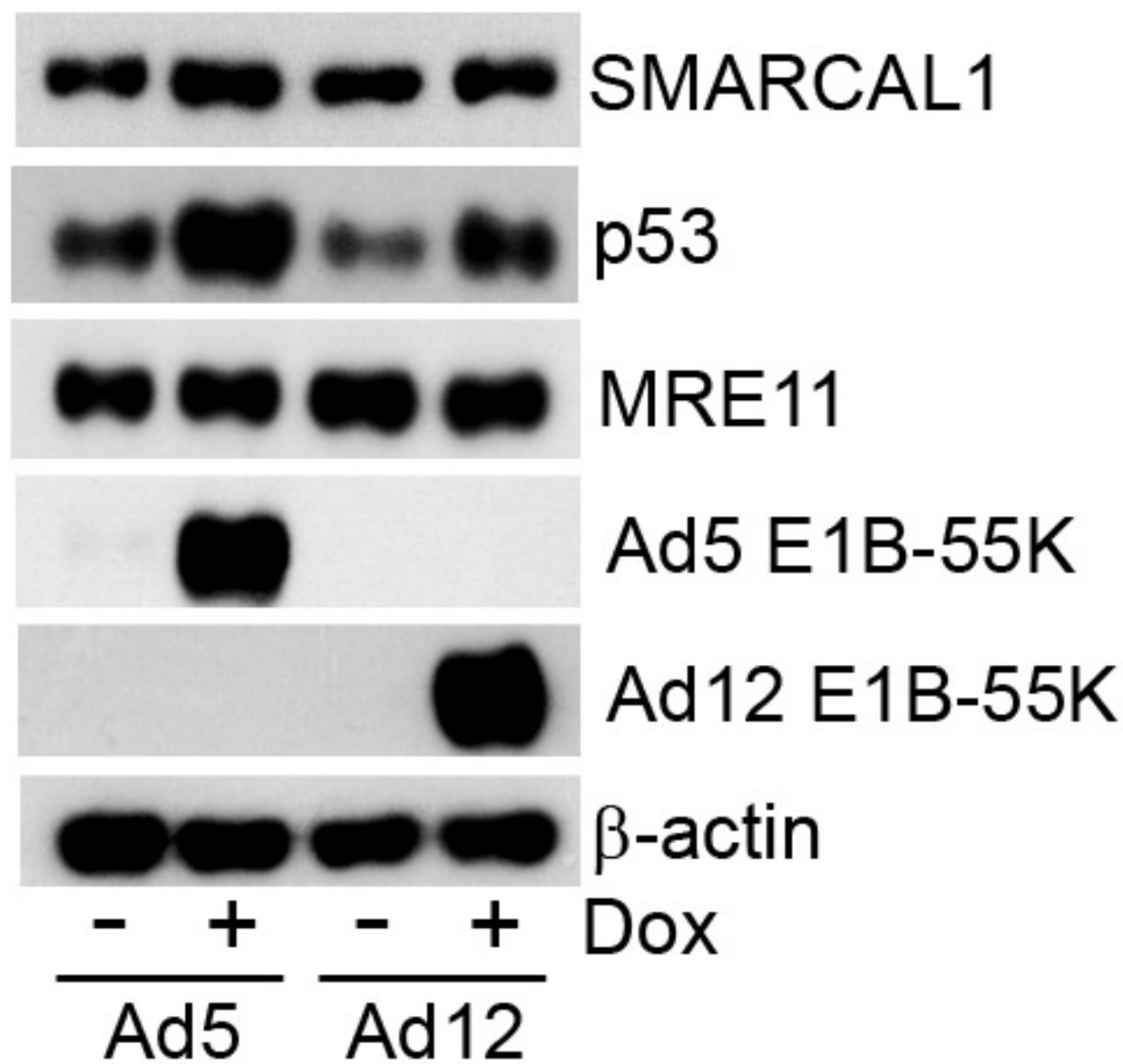


Figure 8

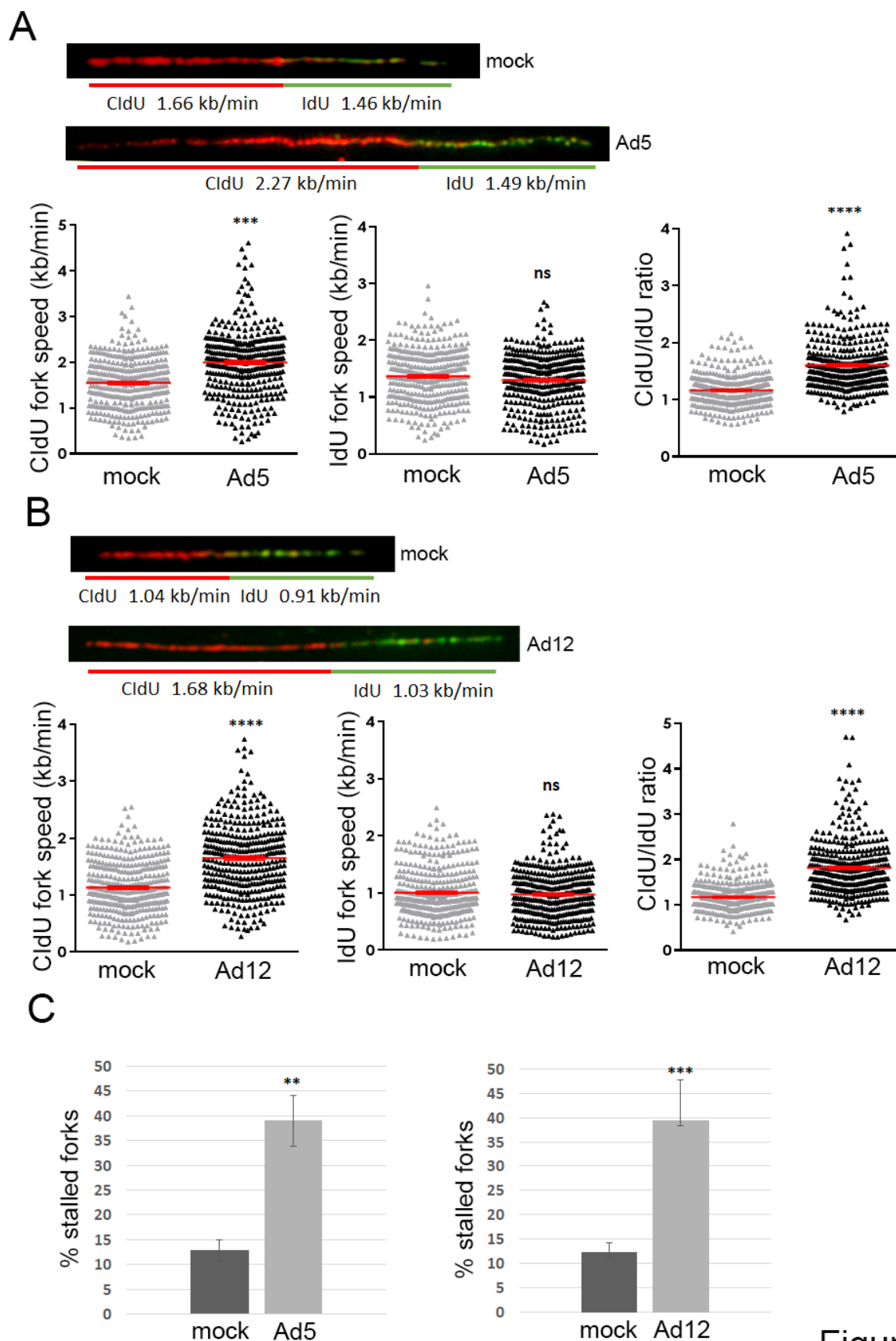


Figure 9